

# Sub-1 nm Nanomaterials Applied in Energy Storage

Guobao Yuan,<sup>[a]</sup> Junli Liu,\*<sup>[a]</sup> and Yu Zhang\*<sup>[a, b]</sup>

Sub-1 nm nanomaterials (SNMs) present rapid electrons/ions transport and unique polymer-analogue properties due to their ultrahigh specific surface area and nearly 100% surface atomic exposure, which are very promising in the application of energy storage devices. However, there still lack of relative review about the SNMs applied in energy storage until now. This review focuses on the structural advantages of SNMs and their synthesis methods, and then discusses latest advances of

employing SNMs for advanced battery systems. The superior functions of SNMs are emphasized for designing every single component in batteries, including electrode materials, separators and electrolytes, greatly improving the performance of batteries. Finally, the current challenges and future research directions of SNMs are proposed, aiming to provide a new insight into the design and manufacture of SNMs for the further development of high-performance energy storage devices.

## 1. Introduction

In recent years, energy storage technologies have made significant development in response to the growing global energy shortage and environmental pollution issues. Among numerous energy storage technologies, rechargeable electrochemical energy storage technology is of particular interest due to its attractive advantages of high energy conversion efficiency, long cycle life, cost effectiveness, environmental friendliness and renewability.<sup>[1]</sup> For example, we have witnessed the fast development of rechargeable lithium-ion batteries (LIBs) over the past 30 years and their widespread application in portable electronic products, such as smartphones, tablets, laptops, and watches.<sup>[2]</sup> Nevertheless, the performance of current commercial LIBs cannot meet the requirements of large-scale energy storage systems for high power density, long cycle life, and high safety.<sup>[3]</sup> Therefore, further improving the performance of LIBs and developing high-performance energy storage devices to surpass LIBs are particularly crucial.

As the indispensable component of battery energy storage devices (electrode materials, separators and electrolytes, etc.), materials always play an important role in the electrochemical performance of batteries. In the past decade, nanomaterials have demonstrated superior performance over their bulk counterparts in battery energy storage applications due to their unique and fascinating properties, such as large specific surface and short electrons/ions transport paths.<sup>[4]</sup> With the continuous development of synthesis and advanced characterization techniques, the exploration of sub-1 nm nanomaterials (SNMs)

between the single-molecule scale and the traditional nanoscale has received extensive attention.<sup>[5]</sup> These SNMs breaking through the traditional nanoscale tend to have larger specific surface areas, more active sites and special properties different from traditional nanomaterials, all of which provide the opportunity to further improve the performance of SNMs for energy storage application.

Generally, SNMs refer to nanomaterials with a feature size of less than 1 nm in at least one dimension, and this feature size is near the size of a single unit cell of many crystals and the diameter of a linear polymer/single DNA chain.<sup>[6]</sup> When the size of nanomaterials decreases into sub-1 nm scale, their properties usually undergo a qualitative leap due to changes in the electronic and energy band structure.<sup>[7]</sup> As shown in Figure 1, SNMs exhibit very fascinating structural advantages for energy storage applications. First, the ultrahigh specific surface area, close to 100% surface atomic exposure and abundant active sites enable SNMs to effectively interact with external fields, which endow SNMs with excellent catalytic and energy conversion properties,<sup>[8]</sup> making them possible to be used as the Li–O<sub>2</sub> or Li–S batteries catalysts.<sup>[9]</sup> Moreover, the special sub-1 nm structures can effectively shorten the electron and ion diffusion distance, increase the electrochemical activity surface area, accelerate electrolyte penetration, alleviate the stress caused by volume expansion and further improve the reaction

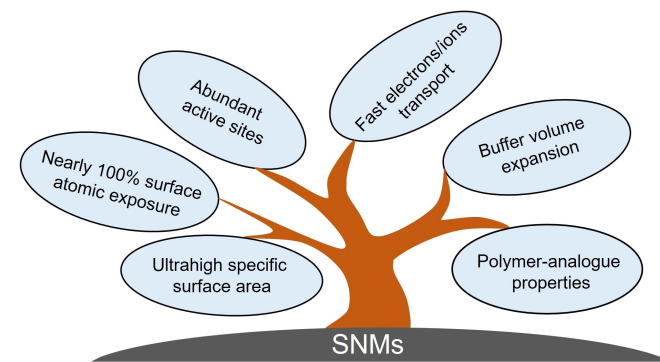


Figure 1. Structural advantages of SNMs for energy storage applications.

[a] G. Yuan, Prof. J. Liu, Prof. Y. Zhang

Key Laboratory of Bio-inspired Smart Interfacial Science and Technology of Ministry of Education  
School of Chemistry, Beihang University  
Beijing 100191 (P. R. China)  
E-mail: liujunli@buaa.edu.cn  
jade@buaa.edu.cn

[b] Prof. Y. Zhang

Beijing Advanced Innovation Center for Biomedical Engineering  
Beihang University  
Beijing 100191 (P. R. China)

kinetics,<sup>[10]</sup> thus leading to high capacity, high rate capability and long cycle life of electrode materials in LIBs or sodium-ion batteries (SIBs). Furthermore, SNMs exhibit polymer-analogue properties, and their assemblies possess excellent structural flexibility, machinability, viscosity and gelation.<sup>[11]</sup> As a result, SNMs can be processed like polymers, which is expected to replace traditional polymer separators and polymer solid-state electrolytes. The above properties make SNMs become the promising components for constructing advanced energy storage devices.

In view of the rapidly increasing interest in SNMs, it is imperative to emphasize their recent advances and development prospects in energy storage. In this review, we emphatically elaborate the structural advantages and synthesis strategies of SNMs, and their crucial role in advanced battery systems. In detail, we summarize and briefly discuss the successful examples of rational design of SNMs as the electrode materials, separators and electrolytes (Figure 2), which demonstrate the great practical application prospects of SNMs in energy storage field. On the basis of previous studies, we finally point out the current challenges and future research directions of SNMs for high-performance energy storage devices.

## 2. Synthesis of SNMs

The reasonable design and controllable fabrication of SNMs are the key prerequisites for their application in energy storage devices. As such, it is imperative to explore simple, clean and efficient fabrication methods to boost the sustainable development of SNMs. Currently, there are various methods for fabricating SNMs, such as hydrothermal/solvothermal method, colloidal-chemical method, template-assisted method, chemical deposition, physical ball-milling, sonication-assisted exfoliation, etc. A few representative examples are listed in Table 1. Here, we mainly discuss solvothermal method.

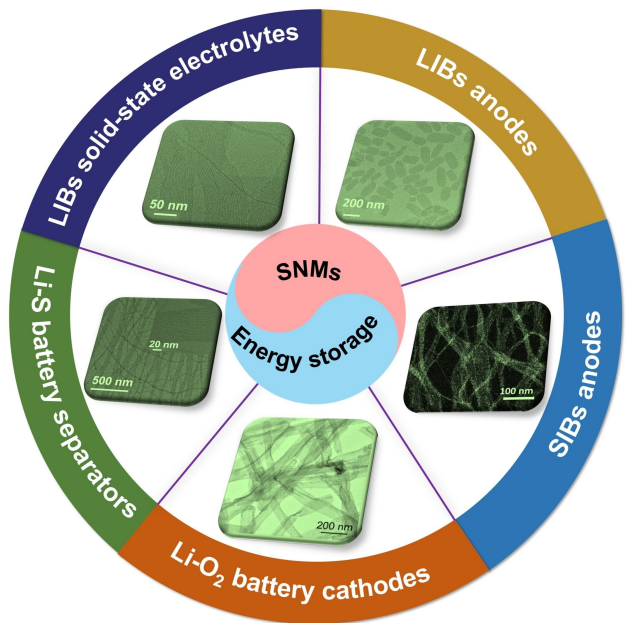
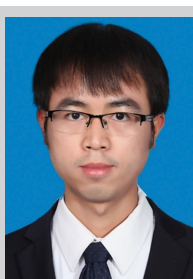


Figure 2. Several typical structures of SNMs and their application in energy storage devices.

Up to now, a variety of SNMs with different dimensions and morphologies have been synthesized, including zero-dimensional (0D) clusters, one-dimensional (1D) sub-1 nm nanowires (SNWs),<sup>[12]</sup> sub-1 nm nanocoils (SNCs)<sup>[13]</sup> and sub-1 nm nanorings (SNRs),<sup>[14]</sup> two-dimensional (2D) sub-1 nm nanobelts (SNBs)<sup>[15]</sup> and sub-1 nm nanosheets (SNSSs).<sup>[16]</sup> Compared to 0D clusters, synthesizing 1D and 2D SNMs presents greater challenges, because the formation of these SNMs requires extreme growth anisotropy in certain dimensions.<sup>[17]</sup> Therefore, it is very important to effectively regulate the interactions between small-sized nuclei formed in the nucleation stage when constructing sub-1 nm structures. Based on this, Wang's



Guobao Yuan received his Bachelor's degree from China University of Geosciences (Beijing) in 2019. He is currently pursuing his Ph.D. degree at Beihang University. His current research interests focus on the design and development of sub-1 nm new-fashioned functional materials for Li/Na-ion, Li–O<sub>2</sub> and Li–S batteries.



Yu Zhang received his Ph.D. degree in Jilin University in 2007. Then he worked as a fellow in New Energy and Industrial Technology Development Organization, Hiroshima University, Japan. He joined Beihang University in 2013 and now is a full professor of the School of Chemistry. He focuses on advanced energy materials, especially for optimizing electrode structures in Li–O<sub>2</sub> and Li/Na-ion battery field.



Junli Liu received her Ph.D. degree in Chemistry from Tsinghua University in 2020. Then she worked as a postdoctor at Tsinghua University from 2020 to 2022. In 2022, she became an associate professor in the School of Chemistry, Beihang University. Her current research focuses on the synthesis, assembly, processing and applications of cluster-based sub-1 nm nanomaterials.

**Table 1.** Materials, nanostructures and fabrication methods reported for SNMs.

Material	Nanostructure	Fabrication methods	Ref.
Tungsten bronze	Sub-1 nm nanowires	One-pot solvothermal method	[20]
GdOOH	Sub-1 nm nanowires	One-pot solvothermal method	[18b, 21]
Indium sulfide	Sub-1 nm nanocoils	One-pot solvothermal method	[18a]
Tungsten oxide	Sub-1 nm nanobelts	One-pot solvothermal method	[22]
MoS <sub>2</sub>	Sub-1 nm nanosheets	One-pot solvothermal method	[23]
Metal oxide-POM	Sub-1 nm nanosheets	One-pot solvothermal method	[16, 24]
Metal oxide-POM	Sub-1 nm nanobelts	One-pot solvothermal method	[15, 25]
POM-based SNWs	Sub-1 nm nanowires	One-pot solvothermal method	[6a, 6b, 8b, 12, 26]
MoO <sub>3-x</sub>	Sub-1 nm nanowires	One-pot hydrothermal method	[27]
Mo/Co(OH) <sub>2</sub>	Sub-1 nm nanosheets	Soft-template method	[28]
HEA-PtPdIrRuAuAg	Sub-1 nm nanobelts	Template-assisted method	[9]
PtIr	Sub-1 nm nanowires	Colloidal-chemical method	[29]
Fe <sub>x</sub> -NOC	Sub-1 nm nanoparticles	Atomic layer deposition	[30]
Au–Ag–Cu	Sub-1 nm nanoparticles	Atom-hybridization method	[31]
Chitin	Sub-1 nm nanobelts	The top-down liquid exfoliation method	[32]
MoS <sub>2</sub> , WS <sub>2</sub> and Graphene	Sub-1 nm nanoparticles	Silica-assisted ball-millin and sonication-assisted exfoliation	[33]

group has realized the preparation of various SNMs in good/poor solvent system,<sup>[13,18]</sup> and proposed the “cluster-nuclei co-assembly” (CNCA) strategy to realize the regulation of inorganic material components at the sub-1 nm scale.<sup>[19]</sup>

In the good/poor solvent system,<sup>[5a]</sup> the good solvent can disperse the product well, while the poor solvent can hardly disperse the product. Thus, the good solvents provide a favorable environment for the growth of nanocrystals. For the poor solvents, they would decrease the supersaturation of the system and accelerate the burst nucleation, which can effectively control the size of the nuclei in the initial stage and simultaneously strengthen the interaction between nuclei to facilitate the formation of sub-1 nm structure. The efficient synthesis of SNMs can be achieved by tuning the species and ratios of good solvent and poor solvent. At the same time, the ligands used in this kind of solvent system, such as oleylamine, often play an important role in precisely regulating the size and morphology of SNMs: they not only act as capping agents to prevent the aggregation of SNMs, but also promote or restrict the growth of nanocrystals in certain dimensions, thereby constructing SNMs with fine structures. Taking the synthesis of tungsten bronze SNWs (TBSNWs) as a typical example to illustrate the feasibility of this method. Wang et al. have synthesized TBSNWs through a one-pot solvothermal method.<sup>[20]</sup> In the experiment, Na<sub>2</sub>WO<sub>4</sub>·2H<sub>2</sub>O and alkali carbonate were first dissolved in water, and oleylamine was dissolved in cyclohexane, in which water served as the poor solvent, cyclohexane and oleylamine served as the good solvent. When these two solvents were mixed, some tungsten oxide clusters generated and oleylamine adsorbed on the surface of the clusters under the high temperature and pressure, then the alkali metal ions entered the surface of the clusters to induce the formation of nuclei. With the increase of reaction time, the amount of oleylamine adsorbed increased,

and oleylamine acted as soft template to guide the formation of SNWs. Many different kinds of SNMs have been successfully fabricated based on good/poor solvents systems, such as GdOOH SNWs,<sup>[18b,21]</sup> indium sulfide SNCs,<sup>[18a]</sup> Co(OH)<sub>2</sub> single-walled nanotube,<sup>[34]</sup> tungsten oxide SNBs,<sup>[22]</sup> MoS<sub>2</sub> SNSs,<sup>[23]</sup> etc.

On the basis of the good/poor solvent system, the CNCA strategy was proposed.<sup>[19]</sup> In this strategy, polyoxometalate (POM) clusters with sizes close to 1 nm and well-defined structures are introduced into the synthetic system of inorganics to intervene the nucleation process, thereby limiting the size of nuclei into the sub-1 nm level. The key determinant of successful co-assembly into sub-1 nm architectures is the matchable sizes of POM clusters and nuclei. As depicted in Figure 3a (left) and 3b, POM clusters with the size near 1 nm are introduced to interact with the monomers at the nucleation stage. Under the effect of POM clusters, the size of inorganic nuclei is successfully limited into the sub-1 nm scale. Due to the size of POMs and nuclei is comparable, it is easy for them to further interact and co-assemble into the co-assembly of cluster and nuclei, which could act as the building block to continue to assemble and grow into various dimensional nanomaterials with sub-1 nm nanostructures. While in the traditional LaMer pathway (Figure 3a (right) and 3c), the size and shape of materials is determined by the nuclei and surrounding monomers. For these two pathways, the difference is that for the CNCA strategy, the introduction of POM clusters can limit the size of nuclei into the sub-1 nm scale at the nucleation stage under the size effect of POMs, which is an important factor for the formation of a series of sub-1 nm structures. As for LaMer pathway, the size of nuclei is influenced by the surrounding monomers (solvents, ligands, etc.) at the nucleation stage, which makes it difficult to control the size of nuclei into the sub-1 nm scale, resulting in the generation of bigger nanomaterials with various morphologies. It is worth mentioning

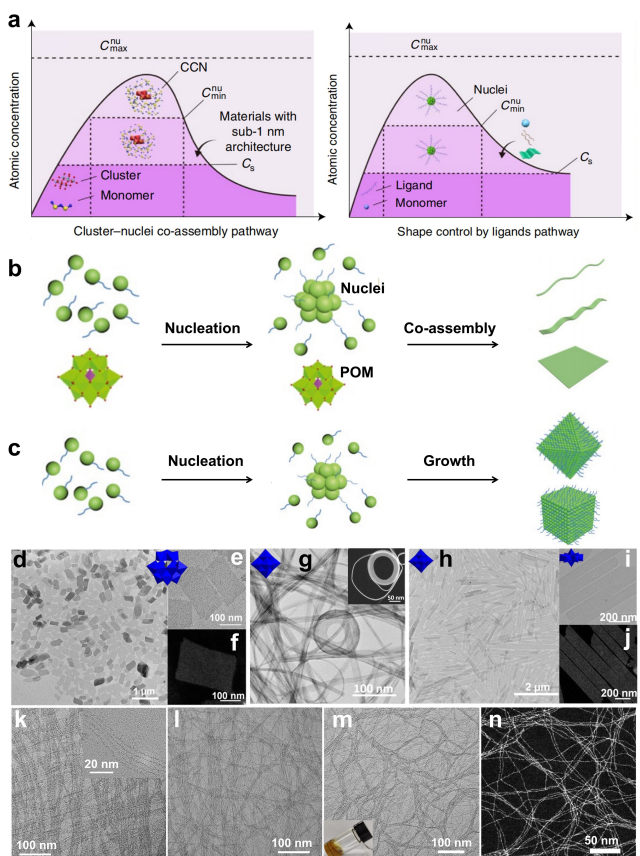


**Figure 3.** (a) Diagram of two different pathways for forming the nanomaterials: the CNCA pathway (left) and the shape control by ligands pathway following the LaMer model (right). Schematic illustration of (b) the CNCA pathway and (c) LaMer pathway. Produced from Ref. [19]. Copyright (2019), with permission from Springer Nature. (d, e) TEM images and (f) HAADF-STEM image of CuO-PMA SNSs. Produced from Ref. [24a]. Copyright (2019), with permission from American Chemical Society. (g) The TEM image and HAADF-STEM image (inset) of MoO<sub>3</sub>-POM SNBs. Produced from Ref. [15]. Copyright (2020), with permission from American Chemical Society. (h, i) TEM images and (j) HAADF-STEM image of ZnO-POM SNSs. Produced from Ref. [16]. Copyright (2021), with permission from American Chemical Society. (k) TEM image and HRTEM image (inset) of Au-PW<sub>12</sub> SNWs. Produced from Ref. [6a]. Copyright (2021), with permission from Wiley-VCH. (l) TEM image of Ni(OH)<sub>2</sub>-PMA SNWs. Produced from Ref. [8b]. Copyright (2021), with permission from American Chemical Society. (m) TEM image of CeO<sub>x</sub>-PMA SNWs (the inset is the corresponding CeO<sub>x</sub>-PMA gel image). Produced from Ref. [12]. Copyright (2022), with permission from American Chemical Society. (n) HAADF-STEM image of CZCNFZC-PMA-Pd SNWs. Produced from Ref. [6b]. Copyright (2023), with permission from Chemical Research in Chinese Universities.

that in CNCA method, the electron-rich nature of POMs is advantageous for their interaction with metal cations driven by noncovalent interactions. Therefore, POMs can serve as carriers and linkers for various metal oxides, which facilitates the directional attachment of building blocks to generate SNMs with highly ordered structures. At present, this strategy has been developed as a general route for the preparation of various component SNMs via a simple one-step solvothermal method. Many SNMs have been successfully fabricated, such as CuO-PMA SNSs (Figure 3d-f),<sup>[24a]</sup> MoO<sub>3</sub>-POM SNBs (Figure 3g),<sup>[15]</sup> ZnO-POM SNSs (Figure 3h-j),<sup>[16]</sup> and a series of POM-based SNWs (e.g., “A-B-A-B” type copolymer-analogue Au-PW<sub>12</sub>

(Figure 3k),<sup>[6a]</sup> Ni(OH)<sub>2</sub>-PMA (Figure 3l),<sup>[8b]</sup> CeO<sub>x</sub>-PMA (Figure 3m)<sup>[12]</sup> and even high-entropy metal oxides CZCNFZC-PMA-Pd SNWs (Figure 3n)<sup>[6b]</sup>, etc.

### 3. Application of SNMs in Energy Storage Devices

It is well known that electrode materials, separators and electrolytes are the core components of a typical battery energy storage system, and their performance directly determines the performance of the battery, such as capacity and cycle life. The design and synthesis of SNMs has opened a new door for battery energy storage materials. As mentioned in the introduction part, the greatest application advantages of SNMs are to provide shorter carrier movement paths, faster migration and transportation rates, which greatly improves the electrochemical reaction kinetics and results in a qualitative leap in battery performance. In the following part, we will present several successful examples of these SNMs that have been used in LIBs, SIBs, Li-O<sub>2</sub> batteries and Li-S batteries.

#### 3.1. SNMs for electrodes

In anode materials, transition metal oxides (TMOs) based on conversion or alloying mechanisms have become a research hotspot for next-generation high-performance LIBs and other advanced battery anode materials due to their high theoretical capacities and low-cost.<sup>[35]</sup> However, during the process of the conversion or alloying reactions, the dramatic volume expansion tends to rupture or even pulverize the structure of the active materials,<sup>[36]</sup> resulting in electrical contact loss and rapid capacity decay.

In this regard, attempts have been made to circumvent these problems by designing sub-1 nm structures. For example, based on the CNCA strategy, we have successfully constructed a novel and stable 2D MnZnCuO<sub>x</sub>-phosphomolybdic acid hybrid sub-1 nm nanosheets (MZC-PMA HSNSs) (Figure 4a-e) by introducing PMA clusters into the TMOs synthesis system and accurately controlling the amount of PMA.<sup>[24c]</sup> As shown in Figure 4f, PMA clusters were introduced to intervene the nucleation of three kinds of TMOs (MnO, ZnO, CuO) and they interacted and co-assembled into the co-assembly, which could act as the building block to continue to grow into the HSNSs. Molecular dynamics (MD) simulations (Figure 4g) have disclosed that PMA clusters interact with TMOs to co-assemble into the 2D HSNSs driven by the electrostatic interaction (Coul) and van der Waals interaction (LJ), and such non-covalent interactions between PMA and TMOs endow the 2D HSNSs with excellent structural and chemical stability, which facilitates the electrochemical reaction of the active materials in the batteries. Meanwhile, the sub-1 nm structure could promote the rapid penetration of electrolytes into the internal region of the electrode, and reduce the path length for electron and ion transport. Also, the sub-1 nm structure can decrease the impact

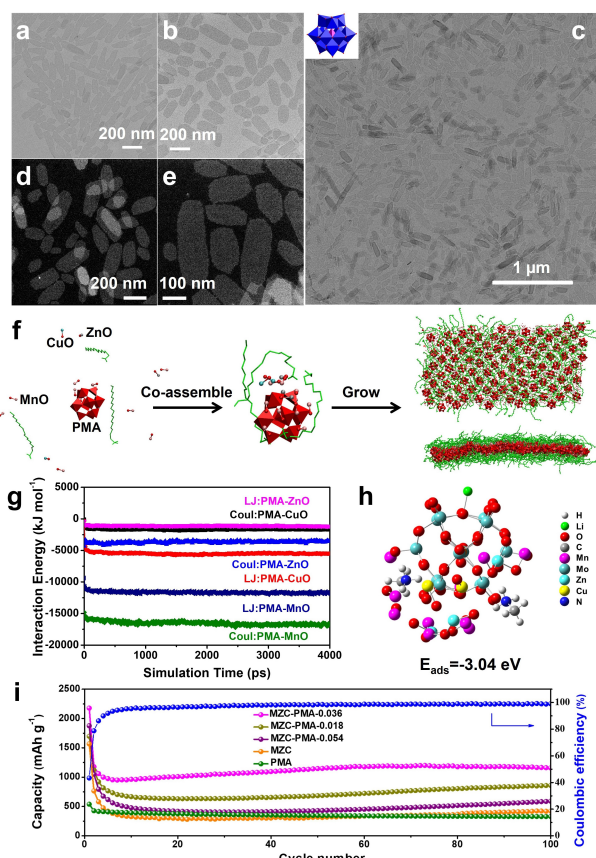


**Figure 4.** (a–c) TEM images of the MZC-PMA HSNSs (the inset is the PMA model). (d, e) HAADF-STEM images of the MZC-PMA HSNSs. (f) Schematic illustration of the formation of MZC-PMA HSNSs. (g) The interaction energy change between PMA and metal oxides in the equilibrium stabilization process of the nanosheet. (h) Li-ions adsorption energy for MZC-PMA-0.036 HSNSs. (i) Long-term cycling tests of MZC-PMA-0.018, MZC-PMA-0.036, MZC-PMA-0.054, MZC and PMA at  $100 \text{ mA g}^{-1}$ . Produced from Ref. [24c]. Copyright (2023), with permission from Wiley-VCH.

of stress caused by volume expansion on the electrode structure, thereby effectively ensuring the high stability of the electrode structure. Notably, the introduction of electron-rich properties of PMA greatly increases the Li-ions adsorption energy on the surface of HSNSs ( $-3.04 \text{ eV}$ ), as confirmed by DFT theoretical calculations (Figure 4h), further promoting the rapid migration of Li-ions within the electrode. All of the components of MZC-PMA HSNSs enhance the reaction kinetics synergistically and thus show excellent electrochemical performance in LIBs. As displayed in Figure 4i, it could deliver a high reversible specific capacity of  $1157 \text{ mAh g}^{-1}$  at  $100 \text{ mA g}^{-1}$  over 100 cycles. Even at  $1000 \text{ mA g}^{-1}$ , an excellent long-term cycling life with a high capacity of  $592 \text{ mAh g}^{-1}$  could be achieved after 700 cycles.

For another instance, we have realized the controllable incorporation of various incompatible metal oxides assisted by POMs clusters, resulting in many high entropy oxides-POM (HEO-POM) SNWs with highly ordered structures,<sup>[12]</sup> as shown in Figure 5a–e. These obtained HEO-POM SNWs have subsequently been used as the novel anode materials in SIBs. The properties of HEO-POM SNWs are not just the sum of the

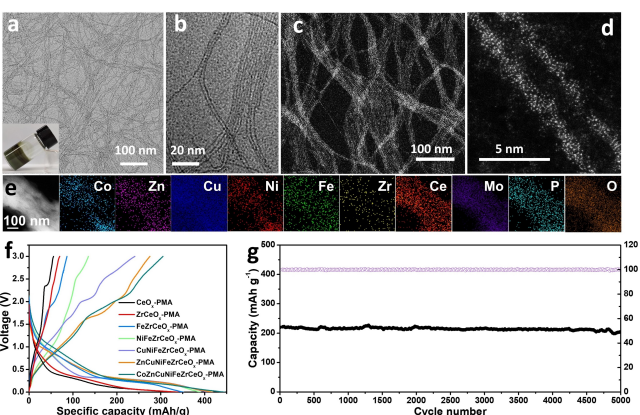


**Figure 5.** (a, b) TEM images, (c) HAADF-STEM image and (d) AC-TEM image of the CoZnCuNiFeZrCeO<sub>x</sub>-PMA SNWs (the inset in (a) is the corresponding HEO-POM gel image). (e) The HAADF-STEM image and EDS element mapping images of the CoZnCuNiFeZrCeO<sub>x</sub>-PMA SNWs. (f) Galvanostatic initial discharge/charge curves for all kinds of HEO-POM SNWs at  $0.1 \text{ C}$ . (g) Cycling stability of the CoZnCuNiFeZrCeO<sub>x</sub>-PMA SNWs at  $10 \text{ C}$ . Produced from Ref. [12]. Copyright (2022), with permission from American Chemical Society.

properties of each metal oxide, but more importantly, the unique sub-1 nm structures and the synergistic effects among the components produce unexpected and unpredictable performance. With the gradual increase of entropy, these SNWs shows better electrochemical performance in SIBs. The reversible specific capacities and corresponding initial columbic efficiencies at  $0.1 \text{ C}$  gradually increase from CeO<sub>x</sub>-PMA ( $56 \text{ mAh g}^{-1}/16.8\%$ ) to CoZnCuNiFeZrCeO<sub>x</sub>-PMA ( $305 \text{ mAh g}^{-1}/68.4\%$ ) (Figure 5f). Encouragingly, the CoZnCuNiFeZrCeO<sub>x</sub>-PMA SNWs exhibit superior long-term cycle stability with a good capacity retention of  $\sim 92\%$  after 5000 cycles even at  $10 \text{ C}$  (Figure 5g). Such entropy modulation strategy provides a promising approach to improve the specific capacity and cycling stability of electrodes.

Apart from anode materials, SNMs can also serve as cathode catalysts in batteries. As reported, the ultrathin 2D nanostructures, especially 2D sub-1 nm structures, with ultrahigh specific surface area, close to 100% surface atomic exposure and abundant active sites, are considered ideal structures for designing advanced catalysts.<sup>[24b,37]</sup> In view of this, Guo's group has synthesized 2D high-entropy alloys (HEA) SNBs (Figure 6a–f) consisting of 5–8 kinds of metallic elements by using Ag nanowires as the templates.<sup>[9]</sup> In such design, the controllable nucleation and growth of different composition metals on the template were achieved through galvanic exchange reaction and co-reduction process in the wet-chemical synthesis, with a final dealloying strategy capable of removing inner Ag core (Figure 6g). As a cathode catalyst for Li–O<sub>2</sub> batteries, the senary HEA-PtPdIrRuAuAg SNBs exhibited excellent performance with a low charge overpotential of  $0.49 \text{ V}$  (Figure 6h), a good rate performance (Figure 6i) and a long-term cycle life of 100 cycles at  $0.50 \text{ A g}^{-1}$  with a limited capacity of  $1000 \text{ mAh g}^{-1}$  (Figure 6j). The superior electrochemical performance of HEAs can be attributed to the strong reduction ability from high-concen-

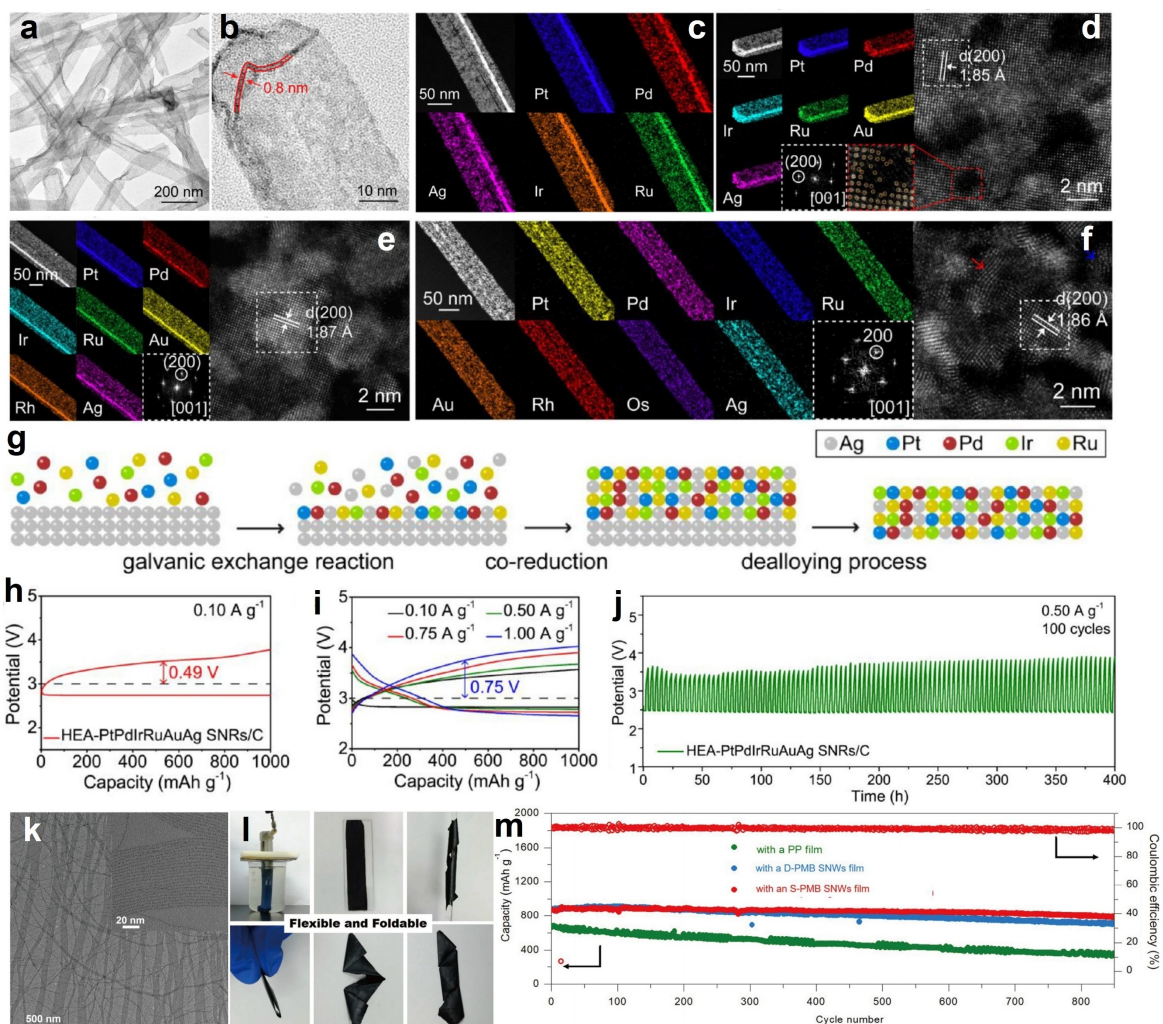


**Figure 6.** (a) Low-magnification and (b) High-magnification TEM images of HEA-PtPdIrRuAg SNB. HAADF-STEM images and EDS element mapping images of (c) HEA-PtPdIrRuAg, (d) HEA-PtPdIrRuAuAg, (e) HEA-PtPdIrRuAuRhAg and (f) HEA-PtPdIrRuAuRhOsAg SNBs. (g) Schematic illustration of mechanism and generality for synthesis of HEA SNRs. (h) Discharge-charge curves of the HEA-PtPdIrRuAuAg SNRs/C at 0.10 A g<sup>-1</sup> with a limited capacity of 1000 mA h g<sup>-1</sup>. (i) Rate performance of the HEA-PtPdIrRuAuAg SNRs/C. (j) Cycling stability of the HEA-PtPdIrRuAuAg SNRs/C at 0.50 A g<sup>-1</sup> with a limited capacity of 1000 mA h g<sup>-1</sup>. Produced from Ref. [9]. Copyright (2023), with permission from American Chemical Society. (k) TEM images of the PMB SNWs. (l) Preparation process of free-standing PMB SNWs films. (m) Long-term cycling tests of Li–S batteries with S-PMB SNWs film, D-PMB SNWs film and PP film at 2 C. Produced from Ref. [26a]. Copyright (2021), with permission from Springer Nature.

tration reductive elements (Pd, Pt, Ag, Au), while the additional elements ensure efficient site-to-site electron transfer.

### 3.2. SNMs for separators

Although Li–S batteries have a high theoretical capacity (1672 mA h g<sup>-1</sup>), their practical application is hindered by the notorious lithium polysulfide shuttling (LPS) and sluggish sulfur conversion kinetics.<sup>[38]</sup> As we all know, the polymer PP films are widely used as Li–S battery components, but the poor electrocatalytic properties of the polymer, and the weak interaction between the polymer and LPS, have largely impeded the improvement of battery performance.<sup>[26a]</sup> Therefore, the development of functional separators seems to be an effective way to improve Li–S battery performance. Considering the polymer-

analogue properties of inorganic SNMs, such as high viscosity, high flexibility, film-forming, processability and gelation, Wang's group further processed the prepared SNWs into free-standing films by using a simple wet-spinning method, which were then used as the separator for Li–S batteries to replace traditional PP polymer separators.

As shown in Figure 6k, Wang's group first fabricated Bi<sub>2</sub>O<sub>3</sub>-POM (PMB) SNWs with curved morphology and high flexibility through a solvothermal method based on the CNCA strategy.<sup>[26a]</sup> After that, they prepared the polymer-resembling films with super-aligned PMB (S-PMB) SNWs via a wet-spinning method, and the free-standing films could fold under different bending degrees without any cracks (Figure 6l), indicating their excellent mechanical flexibility. The obtained film was directly served as an interlayer of Li–S batteries, in which the POM clusters could act as Lewis acids to accept electrons from LPS-Lewis base for

**Table 2.** Comparison of electrochemical performance of SNMs with reported nanomaterials in secondary batteries.

Material	Reversible capacity [(mAh g <sup>-1</sup> )/(mA g <sup>-1</sup> )]	Rate capability [(mAh g <sup>-1</sup> )/(A g <sup>-1</sup> )]	Cycling performance [(mAh g <sup>-1</sup> )/(A g <sup>-1</sup> )/cycles]	Ref.
<b>LIBs</b>				
MnZnCuO <sub>x</sub> -PMA-0.036 sub-1 nm nanosheets	1157/100	615/1.0 474/2.0 377/3.0	592/1.0/700 212/3.0/4000	[24c]
MnO/PC particles	868/100	487/0.7	758/0.3/500	[44]
C@CuO microspheres	626/100	329/3.0	553/1.0/600	[45]
ZnO/CNF-0.5 nanofibers	723/100	175/2	-	[46]
triple-shelled ZnMn <sub>2</sub> O <sub>4</sub> microspheres	641/100	405/1.0	537/0.4/150	[47]
ZnMnO <sub>3</sub> nanotube arrays	860/100	364/2.0	858/0.5/200	[48]
MnO@ZnMn <sub>2</sub> O <sub>4</sub> /N-C nanorods	803/100	464/2.0	595/1.0/200	[49]
<b>SIBs</b>				
CoZnCuNiFeZrCeO <sub>x</sub> -PMA sub-1 nm nanowires	305/30	220/3.0	220/3.0/5000	[12]
CuO nanorod arrays	560/20	200/1.0	291/0.2/460	[50]
Co <sub>3</sub> O <sub>4</sub> particles	245/25	-	447/0.025/50	[51]
α-MoO <sub>3</sub> nanobelts	545/100	188/1.0	280/0.1/50	[52]
SnSe@C microrod	700/100	240/2.0	284/1.0/500	[53]
Fe <sub>2</sub> O <sub>3</sub> @GNS nanocomposite	410/100	110/2.0	400/0.1/200	[54]
<b>Li–O<sub>2</sub> Battery</b>				
Material	Discharge capacity (mAh g <sup>-1</sup> )	Charge overpotential (V)	Cycling performance [cycles / Cutoff capacity (mAh g <sup>-1</sup> ) / (A g <sup>-1</sup> )]	Ref.
HEA-PtPdIrRuAuAg sub-1 nm nanobelts	5252	0.49	100/1000/0.5	[9]
NiO–RuO <sub>2</sub> /KB nanoparticles	4600	0.95	50/1000/0.4	[55]
PtRu nanoparticles	3689	1.09	120/1000/0.5	[56]
NiCo <sub>2</sub> O <sub>4</sub> /La <sub>0.8</sub> Sr <sub>0.2</sub> MnO <sub>3</sub> nanorods	7992	1.12	80/1000/0.2	[57]
NiO nanosheets	1260	0.99	40/500/0.1	[58]
<b>Li–S Battery</b>				
Material	Sulfur loading (mg cm <sup>-2</sup> )	Highest rate/ Capability (mAh g <sup>-1</sup> )	Capability (mAh g <sup>-1</sup> ) / Rate / Cycle / Decay per cycle	Ref.
S-PMB sub-1 nm nanowire separators	1.5	5 C/851	~900/0.5 C/500/0.030 % 782/2 C/850/0.013 % ~600/5 C/1000/0.045 %	[26a]
PAN@APP nanofibers separators	1.8	3 C/507	601/2 C/800/0.021 %	[59]
rGO@SL/PP separators	1.5	2 C/707	523/2 C/1000/0.026 %	[60]
LLZTO separators	1.0	2 C/403	537/0.5 C/500/0.034 %	[61]
<b>Solid-state Battery</b>				
PEO-based composite solid electrolytes	Ionic conductivity (S cm <sup>-1</sup> )/Temperature	Highest rate/Capability (mAh g <sup>-1</sup> )/Temperature	Capability (mAh g <sup>-1</sup> )/Rate/Cycle/Temperature	Ref.
GdOOH sub-1 nm nanowires/ PEO	5.2×10 <sup>-4</sup> /25 °C	2 C/120/60 °C	130/0.5 C/1000/60 °C 115/1 C/700/60 °C	[42]
Mg <sub>2</sub> B <sub>2</sub> O <sub>5</sub> nanowire/PEO	1.53×10 <sup>-4</sup> /40 °C	2 C/72/50 °C	120/1 C/230/50 °C	[62]
MoO <sub>3</sub> nanobelt/PEO	1.16×10 <sup>-3</sup> /60 °C	2 C/120/60 °C	140/0.5 C/350/60 °C	[63]
Ca-doped CeO <sub>2</sub> nanotube/PEO	1.3×10 <sup>-4</sup> /60 °C	2 C/100/60 °C	93/1 C/200/60 °C	[64]
LLZO nanoparticle/PEO	1.05×10 <sup>-4</sup> /50 °C	2 C/131/60 °C	147.6/0.2 C/180/50 °C	[65]

efficient adsorption of LiPS, and  $\text{Bi}_2\text{O}_3$  could promote the interfacial kinetics of LPS liquid-liquid conversion. Benefiting from the strong synergistic effect of the components, the S-PMB SNWs film effectively suppressed the LPS shuttling, accelerated the conversion kinetics of LPS and improved the stability of the Li anode, thereby giving rise to durable battery performance. The Li-S batteries with the PMB SNWs film displayed a high initial specific capacity of  $877 \text{ mAh g}^{-1}$  at 2 C and an excellent cycle stability of  $782 \text{ mAh g}^{-1}$  after 850 cycles with only 0.013% capacity fading per cycle (Figure 6m), which was superior to that of Li-S batteries with PP films. Excitingly, it could cycle up to 1000 times with a low attenuation rate of 0.045% per cycle even at 5 C. These considerable capacity retention ratios enabled by the S-PMB SNWs films lay the foundation for their practical application as a next-generation alternative to PP separators.

### 3.3. SNMs for composite solid-state electrolytes

Solid-state electrolytes have been extensively researched by virtue of their great potential to improve battery energy density and safety.<sup>[39]</sup> Compared with the brittle inorganic solid electrolytes, solid polymer electrolytes (SPEs) have tremendous natural advantages, such as low production cost, easy processability, light weight, flexibility, good elasticity, and ease of film manufacture, therefore holding the most promise for large-scale processing applications.<sup>[40]</sup> However, the low ionic conductivity of SPEs at room temperature makes them difficult to meet the practical application demands of solid-state batteries.<sup>[41]</sup>

Fortunately, the integration of different types of second-phase fillers to the polymer matrix to form composite solid electrolytes (CSEs) has been an effective way to boost the ionic conductivity of SPEs.<sup>[43]</sup> Recently, Mai's group prepared a novel kind of cluster chain/polymer chain composite solid-state electrolyte by dispersing GdOOH SNWs into the polymer matrix.<sup>[42]</sup> The GdOOH SNWs with high length-to-diameter ratio, ultrahigh specific surface area, and abundant surface atomic exposure could bind well with the polymer chains, thus achieving the monodispersion of inorganic cluster chains in the polymer matrix (Figure 7a,b). Compared with the large-size inorganic fillers ( $> 10 \text{ nm}$  or even  $> 100 \text{ nm}$ ), the sub-1 nm cluster chain fillers significantly increased the  $\text{Li}^+$  conductive area at the organic-inorganic interface (Figure 7c). In consequence, the monodisperse cluster chains and the unique sub-1 nm structure were beneficial to provide more interface areas to enhance the space charge layer effect, which could boost the  $\text{Li}^+$  transport in fully active  $\text{Li}^+$  conductive networks. Moreover, these GdOOH SNWs fillers greatly decreased the crystallinity of polymer chains through interacting with the polymer matrix, as verified by XRD (Figure 7d), which was beneficial to reduce the complexation of the polymer with Li-ions and improve the transport efficiency of Li-ions. At the same time, the Lewis acid-base interaction between the inorganic cluster chains surface and  $\text{TFSI}^-$  anions facilitated the Li-salts dissociation and enhanced the Li-ions transport ability (Figure 7e). Furthermore, the interconnected monodisperse cluster chains within the

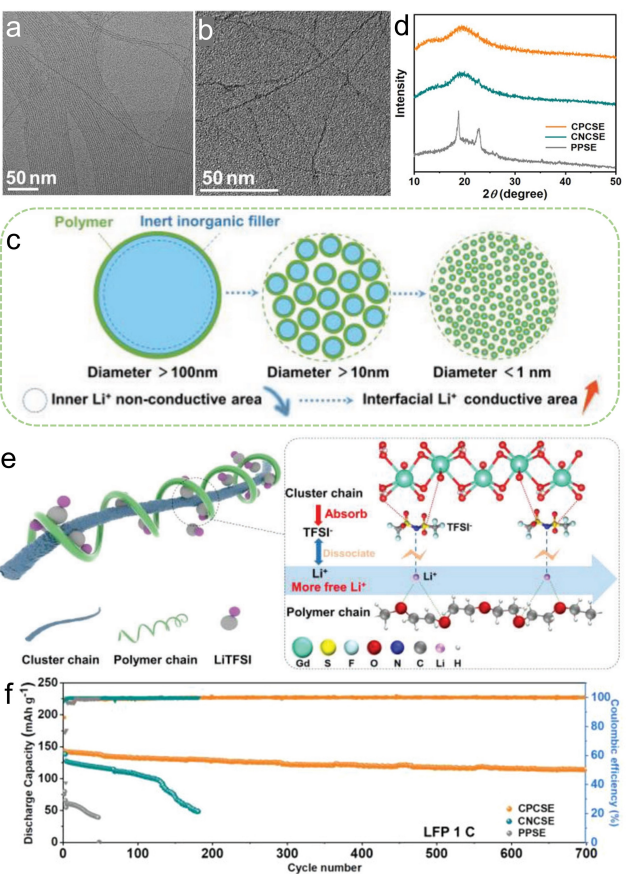


**Figure 7.** (a) The TEM image of the GdOOH cluster chain SNWs. (b) The in-situ liquid TEM image of the cluster chain/PEO/LiTFSI mixed liquid. (c) Schematic illustration of interface areas in CSEs with different size of fillers. (d) The XRD patterns of CPCSE, CNCSE, and PPSE. (e) Schematic illustration of the mechanism for enhanced Li-ions transport in organic-inorganic interface. (f) The cycling performance of the  $\text{LiFePO}_4/\text{Li}$  solid-state battery at 1 C. Produced from Ref. [42]. Copyright (2023), with permission from Wiley-VCH.

polymer matrix could form 3D networks, which could act as expressways for continuous and fast  $\text{Li}^+$  transport channels. Benefiting from the above advantages, the obtained flexible composite solid-state electrolyte membrane exhibited high ion conductivity at room temperature ( $5.2 \times 10^{-4} \text{ S cm}^{-1}$ ), large  $\text{Li}^+$  transference number (0.62), and large distribution area of mobile  $\text{Li}^+$  (50.7%), which was obviously higher than that of pure polymer solid electrolytes. Hence, the assembled  $\text{LiFePO}_4/\text{Li}$  battery could achieve excellent cycle stability of 1000 cycles at 0.5 C with a capacity retention of 87.7% and 700 cycles at 1 C with a capacity retention of 80.2% (Figure 7f). This research work emphasized the importance of sub-1 nm cluster chain as unique fillers for the construction of homogeneous, large-scale, and continuous  $\text{Li}^+$  rapid transport channels, providing a novel strategy to address current bottlenecks in the development of polymer solid-state electrolytes.

## 4. Summary and Outlook

This review summarizes the structural advantages and synthetic methods of SNMs, as well as their recent progress in the application of energy storage devices. In a comprehensive comparison, SNMs exhibit better electrochemical properties than their nano-counterparts, representative examples of which are listed in Table 2. Despite the extraordinary energy storage potential in improving electrochemical performance, there are still issues that need to be addressed for SNMs. To this end, we present the current challenges of SNMs and their future research directions.

- (1) The synthesis of SNMs still faces great challenges. In general, the synthesis of SNMs involves a complex and multi-dimensional chemical reaction system that requires consideration of various reaction conditions, such as pH value, concentration of precursors, additives, solvents, reaction time and temperature, etc. Therefore, it is necessary to optimize the experimental conditions and develop new synthetic methods. Meanwhile, with the development and popularization of machine learning technology, the use of machine learning algorithms to guide the experimental synthesis will be an effective way to enhance the efficiency of finding and designing novel SNMs.
- (2) It should further disclose the deeper mechanisms of the growth process of CNCA strategy, including the principles of ligand interactions and influencing factors controlling the different dimensions of the structures. Moreover, the CNCA strategy is mainly used for the synthesis of metal oxides and hydroxides, and exploring this method for the synthesis of other SNMs, such as sulfides, selenides, phosphides, and high-entropy alloys, is also a future research priority. Furthermore, the clusters utilized in this strategy so far are only POMs, and researching new types of clusters (e.g., metal clusters) to replace POMs would be helpful for constructing novel SNMs.
- (3) At present, the exploration of SNMs for battery energy storage devices is still in its infancy stage. It can be predicted that SNMs have also promising applications in other battery systems, including K/Zn/Mg/Ca/Al-ion batteries, Na/K/Zn/Mg/Al-O<sub>2</sub> batteries, Li/Na/K/Zn/Mg/Al-CO<sub>2</sub> batteries and Na/K/Mg/Ca/Al-S batteries. Given the polymer-analogue properties of SNMs, it has the potential to replace the commercial polymer separators and traditional polymer solid-state electrolytes in the future, and realize the practical application of SNMs in separators and solid-state electrolytes.

In summary, SNMs with unique and intriguing advantages provide a great opportunity to develop high-performance energy storage devices. With the continuous advances in composition design and synthetic strategies, the realization of high-performance SNMs is just around the corner. We firmly believe that with the joint efforts of scientific researchers, the widespread application of SNMs in battery energy storage can be achieved.

## Acknowledgements

J. Liu is thankful for the support from the National Natural Science Foundation of China (Grant No. 22305012). Y. Zhang is thankful for the support from the National Natural Science Foundation of China (Grant No. 51925202 and U22A20141).

## Conflict of Interests

The authors declare no conflict of interest.

**Keywords:** Batteries • Co-assembled • Energy Storage • Polyoxometalate Cluster • Sub-1 nm

- [1] a) J. Zhang, Y. Li, Z. Chen, Q. Liu, Q. Chen, M. Chen, *Energy Environ. Mater.* **2023**, *0*, e12573; b) R. C. K. Reddy, X. Lin, A. Zeb, C.-Y. Su, *Electrochim. Energy Rev.* **2021**, *5*, 312–347; c) B. Akkinapally, I. N. Reddy, V. Manjunath, M. V. Reddy, Y. K. Mishra, T. J. Ko, K. Zaghib, J. Shim, *Int. J. Energy Res.* **2022**, *46*, 14116–14132.
- [2] a) W. Xu, C. Tang, N. Huang, A. Du, M. Wu, J. Zhang, H. Zhang, *Small Sci.* **2022**, *2*, 2100105; b) S. Li, J. Lin, Y. Zhang, S. Zhang, T. Jiang, Z. Hu, J. Liu, D. Y. Wu, L. Zhang, Z. Tian, *Adv. Energy Mater.* **2022**, *12*, 2201347; c) A. A. AbdelHamid, A. Mendoza-Garcia, J. Y. Ying, *Nano Energy* **2022**, *93*, 106860.
- [3] a) S. K. Kang, M. Kim, H. H. Shin, W. Yoon, S. Lee, D. Jang, J. Choi, G. H. Park, J. Park, W. B. Kim, *Adv. Funct. Mater.* **2023**, *33*, 2300143; b) X. Sun, C. Yang, Y. Zhao, Y. Li, Z. Shang, H. Zhou, W. Liu, L. Luo, X. Sun, *Adv. Funct. Mater.* **2022**, *32*, 2109112; c) Z. Zou, Q. Wang, K. Zhu, K. Ye, G. Wang, D. Cao, J. Yan, *Small* **2022**, *18*, 2106673.
- [4] Y. Liu, S. Wang, X. Sun, J. Zhang, F. uz Zaman, L. Hou, C. Yuan, *Energy Environ. Mater.* **2023**, *6*, e12263.
- [5] a) X. Cheng, S. Zhang, X. Wang, *Nano Lett.* **2021**, *21*, 9845–9852; b) S. Zhang, X. Wang, *Acc. Mater. Res.* **2022**, *3*, 1285–1298; c) Q. Liu, X. Wang, *Angew. Chem. Int. Ed.* **2023**, *62*, e202217764.
- [6] a) J. Liu, S. Wang, N. Liu, D. Yang, H. Wang, H. Hu, J. Zhuang, X. Wang, *Small* **2021**, *17*, e2006260; b) J. Liu, S. Nie, L. Wu, X. Wang, *Chem. Res. Chin. Univ.* **2023**, *39*, 624–629; c) B. Ni, Y. Shi, X. Wang, *Adv. Mater.* **2018**, *30*, 1802031.
- [7] a) S. Zhang, X. Wang, *ACS Materials Lett.* **2020**, *2*, 639–643; b) Q. Liu, X. Wang, *InfoMat* **2021**, *3*, 854–868.
- [8] a) J. Liu, M. Wang, M. C. Dipalo, J. Zhuang, W. Shi, X. Wang, *Chem. Sci.* **2021**, *12*, 11490–11494; b) J. Liu, J. Zhuang, W. Shi, X. Wang, *Chem. Mater.* **2021**, *33*, 7100–7105.
- [9] L. Tao, M. Sun, Y. Zhou, M. Luo, F. Lv, M. Li, Q. Zhang, L. Gu, B. Huang, S. Guo, *J. Am. Chem. Soc.* **2022**, *144*, 10582–10590.
- [10] a) J. Li, Q. Meng, Y. Zhang, L. Peng, G. Yu, A. C. Marschilok, L. Wu, D. Su, K. J. Takeuchi, E. S. Takeuchi, Y. Zhu, E. A. Stach, *Nat. Commun.* **2019**, *10*, 93; b) L. Peng, Z. Fang, J. Li, L. Wang, A. M. Bruck, Y. Zhu, Y. Zhang, K. J. Takeuchi, A. C. Marschilok, E. A. Stach, E. S. Takeuchi, G. Yu, *ACS Nano* **2017**, *12*, 820–828.
- [11] a) S. Zhang, W. Shi, X. Wang, *Science* **2022**, *377*, 100–104; b) S. Zhang, X. Wang, *ACS Nano* **2022**, *17*, 20–26.
- [12] J. Liu, Y. Li, Z. Chen, N. Liu, L. Zheng, W. Shi, X. Wang, *J. Am. Chem. Soc.* **2022**, *144*, 23191–23197.
- [13] S. Hu, H. Liu, P. Wang, X. Wang, *J. Am. Chem. Soc.* **2013**, *135*, 11115–11124.
- [14] Q. Liu, P. He, H. Yu, L. Gu, B. Ni, D. Wang, X. Wang, *Sci. Adv.* **2019**, *5*, eaax1081.
- [15] J. Liu, N. Liu, H. Wang, W. Shi, J. Zhuang, X. Wang, *J. Am. Chem. Soc.* **2020**, *142*, 17557–17563.
- [16] J. Liu, W. Shi, X. Wang, *J. Am. Chem. Soc.* **2021**, *143*, 16217–16225.
- [17] S. Rong, X. Wang, *Chem. Commun.* **2022**, *58*, 11475–11487.
- [18] a) P.-P. Wang, Y. Yang, J. Zhuang, X. Wang, *J. Am. Chem. Soc.* **2013**, *135*, 6834–6837; b) H. Liu, Q. Gong, Y. Yue, L. Guo, X. Wang, *J. Am. Chem. Soc.* **2017**, *139*, 8579–8585.
- [19] J. Liu, W. Shi, B. Ni, Y. Yang, S. Li, J. Zhuang, X. Wang, *Nat. Chem.* **2019**, *11*, 839–845.

- [20] S. Zhang, Y. Shi, T. He, B. Ni, C. Li, X. Wang, *Chem. Mater.* **2018**, *30*, 8727–8731.
- [21] a) S. Zhang, W. Shi, T. D. Siegler, X. Gao, F. Ge, B. A. Korgel, Y. He, S. Li, X. Wang, *Angew. Chem. Int. Ed.* **2019**, *58*, 8730–8735; b) S. Zhang, W. Shi, S. Rong, S. Li, J. Zhuang, X. Wang, *J. Am. Chem. Soc.* **2020**, *142*, 1375–1381; c) S. Zhang, H. Lin, H. Yang, B. Ni, H. Li, X. Wang, *Adv. Funct. Mater.* **2019**, *29*, 1903477.
- [22] J. He, H. Liu, B. Xu, X. Wang, *Small* **2014**, *11*, 1144–1149.
- [23] P. P. Wang, H. Sun, Y. Ji, W. Li, X. Wang, *Adv. Mater.* **2014**, *26*, 964–969.
- [24] a) J. Liu, W. Shi, X. Wang, *J. Am. Chem. Soc.* **2019**, *141*, 18754–18758; b) J. Liu, W. Shi, S. Nie, X. Wang, *Small Structures* **2022**, *3*, 2200039; c) G. Yuan, H. Ge, W. Shi, J. Liu, Y. Zhang, X. Wang, *Angew. Chem. Int. Ed.* **2023**, *62*, e202309934.
- [25] S. Zhang, N. Liu, H. Wang, Q. Lu, W. Shi, X. Wang, *Adv. Mater.* **2021**, *33*, 2100576.
- [26] a) S. Zhang, H. Shi, J. Tang, W. Shi, Z.-S. Wu, X. Wang, *Sci. China Mater.* **2021**, *64*, 2949–2957; b) S. Zhang, W. Shi, B. Yu, X. Wang, *J. Am. Chem. Soc.* **2022**, *144*, 16389–16394; c) S. Zhang, W. Shi, X. Wang, *Science* **2022**, *377*, 100–104; d) S. Zhang, Q. Lu, B. Yu, X. Cheng, J. Zhuang, X. Wang, *Adv. Funct. Mater.* **2021**, *31*, 2100703.
- [27] Y. Fang, Y. Yu, X. Jiang, P. Liu, Y. Chen, W. Feng, *Adv. Funct. Mater.* **2023**, *33*, 2304163.
- [28] H. Yang, M. Luo, S. Lu, Q. Zhang, Y. Chao, F. Lv, L. Zhu, L. Bai, L. Yang, W. Wang, D. Wei, Y. Liang, L. Gu, H. Chen, S. Guo, *Chem.* **2022**, *8*, 2460–2471.
- [29] K. Yin, Y. Chao, F. Lv, L. Tao, W. Zhang, S. Lu, M. Li, Q. Zhang, L. Gu, H. Li, S. Guo, *J. Am. Chem. Soc.* **2021**, *143*, 10822–10827.
- [30] F. Bu, C. Chen, Y. Yu, W. Hao, S. Zhao, Y. Hu, Y. Qin, *Angew. Chem. Int. Ed.* **2022**, *62*, e202216062.
- [31] T. Moriai, T. Tsukamoto, M. Tanabe, T. Kambe, K. Yamamoto, *Angew. Chem. Int. Ed.* **2020**, *59*, 23051–23055.
- [32] Y. Ding, X. Chen, Y. Zhou, X. Ren, W. Zhang, M. Li, Q. Zhang, T. Jiang, B. Ding, D. Shi, J. You, *Adv. Sci.* **2022**, *9*, 2201287.
- [33] a) Z. Chen, X. Wu, L. Xiao, H. Gao, Z. Li, X. Zhou, Y. Li, N. Guo, Y. Guo, X. Qi, L. Bai, H. Chang, Q. Zheng, X. Liu, Y. Zhang, *Nano Today* **2024**, *54*, 102126; b) Z. Chen, Y. Zhang, C. Zhao, Y. Xia, Z. Li, X. Zhou, L. Xiao, X. Liu, Y. Zhang, *Adv. Mater.* **2024**, 2310022, DOI: 10.1002/adma.202310022.
- [34] B. Ni, H. Liu, P.-P. Wang, J. He, X. Wang, *Nat. Commun.* **2015**, *6*, 8756.
- [35] a) S. Li, K. Wang, G. Zhang, S. Li, Y. Xu, X. Zhang, X. Zhang, S. Zheng, X. Sun, Y. Ma, *Adv. Funct. Mater.* **2022**, *32*, 2200796; b) Y. Zhang, Y. Xu, Y. Ji, X. Wang, J. Li, H. Liu, D. Wang, Z. Zhong, Y. Bando, F. Su, *Energy Storage Mater.* **2019**, *17*, 242–252.
- [36] a) S. Wang, Y. Hao, K. Zhang, H. Liu, L. Liao, *J. Mater. Chem. A* **2023**, *11*, 24959; b) G. Yuan, D. Liu, X. Feng, Y. Zhang, *ChemPlusChem* **2021**, *86*, 1135–1161; c) G. Yuan, D. Liu, X. Feng, M. Shao, Z. Hao, T. Sun, H. Yu, H. Ge, X. Zuo, Y. Zhang, *Adv. Mater.* **2022**, *34*, 2108985.
- [37] Y. Chen, Z. Fan, Z. Zhang, W. Niu, C. Li, N. Yang, B. Chen, H. Zhang, *Chem. Rev.* **2018**, *118*, 6409–6455.
- [38] X. Zuo, M. Zhen, D. Liu, H. Yu, X. Feng, W. Zhou, H. Wang, Y. Zhang, *Adv. Funct. Mater.* **2023**, *33*, 2214206.
- [39] a) P. Wang, J.-H. Liu, W. Cui, X. Li, Z. Li, Y. Wan, J. Zhang, Y.-Z. Long, *J. Mater. Chem. A* **2023**, *11*, 16539–16558; b) S. K. Sharma, G. Sharma, A. Gaur, A. Arya, F. S. Mirsafi, R. Abolhassani, H.-G. Rubahn, J.-S. Yu, Y. K. Mishra, *Energy Adv.* **2022**, *1*, 457–510.
- [40] a) Y. Guo, S. Wu, Y.-B. He, F. Kang, L. Chen, H. Li, Q.-H. Yang, *eScience* **2022**, *2*, 138–163; b) Y. Zheng, Y. Yao, J. Ou, M. Li, D. Luo, H. Dou, Z. Li, K. Amine, A. Yu, Z. Chen, *Chem. Soc. Rev.* **2020**, *49*, 8790–8839.
- [41] X. Yang, J. Liu, N. Pei, Z. Chen, R. Li, L. Fu, P. Zhang, J. Zhao, *Nano-Micro Lett.* **2023**, *15*, 74.
- [42] Y. Cheng, X. Liu, Y. Guo, G. Dong, X. Hu, H. Zhang, X. Xiao, Q. Liu, L. Xu, L. Mai, *Adv. Mater.* **2023**, *35*, 2303226.
- [43] S. Liu, W. Liu, D. Ba, Y. Zhao, Y. Ye, Y. Li, J. Liu, *Adv. Mater.* **2022**, *35*, 2110423.
- [44] S. Jiang, S. Yun, H. Cao, Z. Zhang, H. Feng, H. Chen, *Sci. China Mater.* **2021**, *65*, 59–68.
- [45] X. Sun, Z. Wang, X. Ai, J. Zhou, *Sci. China Mater.* **2023**, *66*, 3026–3038.
- [46] H. Ning, H. Xie, Q. Zhao, J. Liu, W. Tian, Y. Wang, M. Wu, *J. Alloys Compd.* **2017**, *722*, 716–720.
- [47] J. Xu, H. Zhang, R. Wang, P. Xu, Y. Tong, Q. Lu, F. Gao, *Langmuir* **2018**, *34*, 1242–1248.
- [48] H. Chen, L.-X. Ding, K. Xiao, S. Dai, S. Wang, H. Wang, *J. Mater. Chem. A* **2016**, *4*, 16318–16323.
- [49] M. Zhong, D. Yang, C. Xie, Z. Zhang, Z. Zhou, X. H. Bu, *Small* **2016**, *12*, 5564–5571.
- [50] S. Yuan, X. L. Huang, D. L. Ma, H. G. Wang, F. Z. Meng, X. B. Zhang, *Adv. Mater.* **2014**, *26*, 2273–2279.
- [51] M. M. Rahman, A. M. Glushenkov, T. Ramireddy, Y. Chen, *Chem. Commun.* **2014**, *50*, 5057–5060.
- [52] W. Xia, F. Xu, C. Zhu, H. L. Xin, Q. Xu, P. Sun, L. Sun, *Nano Energy* **2016**, *27*, 447–456.
- [53] F. Kong, Z. Han, S. Tao, B. Qian, *J. Energy Chem.* **2021**, *55*, 256–264.
- [54] Z. Jian, B. Zhao, P. Liu, F. Li, M. Zheng, M. Chen, Y. Shi, H. Zhou, *Chem. Commun.* **2014**, *50*, 1215–1217.
- [55] P. Tan, W. Shyy, M. C. Wu, Y. Y. Huang, T. S. Zhao, *J. Power Sources* **2016**, *326*, 303–312.
- [56] Y. Zhou, Q. Gu, K. Yin, Y. Li, L. Tao, H. Tan, Y. Yang, S. Guo, *Angew. Chem. Int. Ed.* **2022**, *61*, e202201416.
- [57] Y. Luo, F. Lu, C. Jin, Y. Wang, R. Yang, C. Yang, *J. Power Sources* **2016**, *319*, 19–26.
- [58] S. Tong, M. Zheng, Y. Lu, Z. Lin, J. Li, X. Zhang, Y. Shi, P. He, H. Zhou, *J. Mater. Chem. A* **2015**, *3*, 16177–16182.
- [59] T. Lei, W. Chen, Y. Hu, W. Lv, X. Lv, Y. Yan, J. Huang, Y. Jiao, J. Chu, C. Yan, C. Wu, Q. Li, W. He, J. Xiong, *Adv. Energy Mater.* **2018**, *8*, 1802441.
- [60] T. Lei, W. Chen, W. Lv, J. Huang, J. Zhu, J. Chu, C. Yan, C. Wu, Y. Yan, W. He, J. Xiong, Y. Li, C. Yan, J. B. Goodenough, X. Duan, *Joule* **2018**, *2*, 2091–2104.
- [61] H. Qu, J. Ju, B. Chen, N. Xue, H. Du, X. Han, J. Zhang, G. Xu, Z. Yu, X. Wang, G. Cui, *J. Mater. Chem. A* **2018**, *6*, 23720–23729.
- [62] O. Sheng, C. Jin, J. Luo, H. Yuan, H. Huang, Y. Gan, J. Zhang, Y. Xia, C. Liang, W. Zhang, X. Tao, *Nano Lett.* **2018**, *18*, 3104–3112.
- [63] X. Wang, S. Huang, K. Guo, Y. Min, Q. Xu, *Adv. Funct. Mater.* **2022**, *32*, 2206976.
- [64] H. Chen, D. Adekoya, L. Hencz, J. Ma, S. Chen, C. Yan, H. Zhao, G. Cui, S. Zhang, *Adv. Energy Mater.* **2020**, *10*, 2000049.
- [65] M. Zhang, P. Pan, Z. Cheng, J. Mao, L. Jiang, C. Ni, S. Park, K. Deng, Y. Hu, K. K. Fu, *Nano Lett.* **2021**, *21*, 7070–7078.

Manuscript received: December 30, 2023

Revised manuscript received: February 2, 2024

Accepted manuscript online: February 22, 2024

Version of record online: March 8, 2024